Supporting Information

Tsuji et al. 10.1073/pnas.0910106107

SI Text

Electrophysiological Analysis of Safe MEF-iPS–Derived Neurons. We examined the electrophysiological properties of the 38C2 iPS-derived neurons. After 21–28 d of differentiation, 38C2 iPS-PNS– and EB3 ES-PNS–derived neurons were examined electrophysiologically using whole-cell patch clamping. In the current-clamp mode, depolarizing current injections triggered repetitive action potentials in both the 38C2 PNS- (n = 11 of 16) and EB3 ES-PNS– (n = 5 of 7) derived neurons. These action potentials were completely blocked by tetrodotoxin (TTX; 1 μM; Fig. S1*A*), indicating that they were mediated by voltage-gated Na^+ channels. In voltage clamp at −60 mV, when step voltage commands were applied to 38C2 PNS-derived neurons, very rapid inward currents were observed from around −40 mV (Fig. S1 *B*-1 and *B*-2). The transient inward currents were immediately followed by transient outward currents (Fig. S1*B*-1), observed from about −20 mV. These K^+ channel-like transient currents may be responsible for the reduction in the amplitudes of the all-or-none Na^+ currents (Fig. S1*C*). Steady outward currents, similar to those mediated by delayed-rectifier K^+ channels, were also observed (Fig. S1 *B*-1 and *D*). Although we have not yet identified the channels that were responsible for these currents, our findings showed that the 38C2 PNSs produced neuronal cells equipped with functional channels that could generate and modify action potentials.

SI Materials and Methods

Cell Culture and Neural Induction. To culture PNSs, day 6 EBs were dissociated and cultured in suspension at 5×10^4 cells/mL in media hormone mix (MHM) supplemented with B27 and 20 ng/mL FGF-2 (Peprotech) for 7–8 d (1, 2). To culture SNSs, PNSs were dissociated and cultured in the same culture medium for 7–8 d. For further differentiation, neurospheres were plated onto poly-L-ornithine/fibronectin-coated coverslips and cultured without FGF-2 for 5 d. To examine the differentiation efficiency, neurospheres dissociated by TripLE Select (Invitrogen) were plated onto poly-L-ornithine/fibronectin-coated coverslips at 5×10^4 cells/cm^2, cultured without FGF-2 for 5 d, and processed for immunocytochemistry as described previously (1, 2).

Lentivirus Production and Infection of Secondary Neurospheres. High-titer, concentrated stocks prepared by ultracentrifugation and resuspension in Dulbecco's PBS (2.68 mM KCl, 1.47 mM KH_2PO_4, 136.89 mM NaCl, and 8.1 mM Na_2HPO_4) were added to the culture medium in which SNSs were formed from EB3 ES, 38C2 PNSs (multiplicity of infection, MOI = 1.0). To prelabel the grafted cells in the case of 335D1 TTF-iPS-SNS, we used lentivirus to transduce mRFP into 335D1 PNSs by modified lentivirus vectors pCSII-EF-mRFP (3).

Electrophysiology. For electrophysiological analysis, EB3 ES or 38C2 PNSs were plated on poly-L-ornithine/fibronectin-coated coverslips and allowed to differentiate for 21–28 d. The cells with a neuron-like morphology were identified under an inverted microscope (Diaphot-TMD 200; Nikon), and whole-cell patch clamp recording was performed at room temperature using an Axopatch 200B (Axon Instruments). The cultured cells were continuously perfused with an external solution containing (in mM) 150 NaCl, 2.5 KCl, 2 $CaCl_2$, 1 $MgCl_2$, 10 D-glucose, and 10 Hepes (pH 7.4 adjusted with NaOH, 310 mOsm). Patch pipettes had a resistance of 10–15 MΩ when filled with pipette solution composed of (in mM) 130 K-gluconate, 1 $CaCl_2$, 1 $MgCl_2$, 10 EGTA, 10 sucrose, and 10 Hepes (pH 7.4 adjusted with KOH, 280 mOsm). Capacitance and series resistance were compensated, and the liquid junction potential was corrected. Cultured cells were held at −60 mV, and voltage steps were applied (10 mV, 150 ms) from −90 mV to 40 mV to elicit voltage-activated currents. The peak amplitudes of the inward currents and the steady-state current amplitudes were plotted against the step-voltage commands. Action potentials were evoked by injecting step currents (25 pA, 150 ms) in the current-clamp mode. TTX (Sankyo Co. Ltd.) was added to the external solution to block action potentials. Signals were filtered at 5 kHz and digitized at 20 kHz (Digidata 1200; Axon Instruments).

Transplantation into Intact and Injured Spinal Cord. The transplantation of lentivirally transduced iPS- and ES-SNSs was performed using a glass micropipette configured to a stereotaxic injector (KDS 310; Muromachi Kikai). Transplantation into the intact spinal cord of C57BL6 female mice was conducted after laminectomy without the induction of spinal cord injury (Fig. S3; 38C2 SNS, n = 2; EB3 SNS, n = 2). For transplantation into the injured spinal cord, the injured site was again exposed 9 d after the injury, and 5×10^5 cells of 38C2 PNSs/SNSs; 335D1, 256H13, or 256H18 iPS-SNSs; EB3 or 1A2 ES-SNSs; or adult dermal fibroblasts in 2 μL of cell suspension were transplanted into the lesion epicenter at a rate of 0.5 μL/min. In the vehicle-control group, PBS was injected instead of SNSs into the lesion site 9 d after the injury.

Bioluminescent Imaging. A Xenogen-IVIS 100 cooled CCD optical macroscopic imaging system (SC BioScience) was used for BLI, as reported previously (4). To quantify the photon counts, we defined a ROI over the cell-implanted area and examined the same ROI in all of the animals. The obtained photon count intensity was expressed as a percentage of the initial value.

Histological Analyses. Grafted animals were deeply anesthetized and intracardially perfused with 4% paraformaldehyde (pH 7.4). The dissected spinal cords were postfixed for 3 h in 4% PFA, soaked overnight in 10% followed by 30% sucrose, embedded in optimal cutting temperature (OCT) compound, and sectioned into 20-μm axial/sagittal sections using a cryostat. Hematoxylin and eosin (H&E) staining was carried out for general histological examination. To examine the distribution of 38C2 SNSs grafted into intact or injured spinal cords, the sections were immunostained with an anti-RFP antibody and visualized with diaminobenzidine (DAB) solution. The phenotypes of the grafted cells were assessed by fluorescent double-immunostaining with antibodies against RFP and one of the cell-type-specific markers listed in Table S2. Images were obtained by fluorescence microscopy (Axioskop 2 plus; Carl Zeiss, and BZ-9000; KEYENCE Co.) or confocal microscopy (LSM510; Carl Zeiss). To quantify the proportion of each phenotype in vivo, we selected five representative midsagittal sections and captured five regions within 500 μm rostral and caudal to the lesion epicenter randomly at 200× magnification. RFP-positive engrafted cells as well as each phenotypic marker-positive cells were counted in each section. To quantify the $5HT^+$ fibers after 38C2 SNS transplantation, we selected five representative axial sections from each animal (38C2 SNS group, n = 3; PBS control group, n = 3), randomly captured 10 regions in each axial section 4 mm caudal to the epicenter at 200× magnification, and quantified the total $5HT^+$ area using the MCID system equipped with a CCD camera (DXC-390; Sony).

Transplantation into the Brain of NOD/SCID Mice. The transplantation of neurospheres lentivirally transduced with Venus (pCSII-EF-MCS-IRES2-Venus) (3) was performed using a glass micropipette

fitted to a stereotaxic injector as described previously (5). The tip of the micropipette was inserted into the right striatum (2 mm lateral, 1 mm rostral to bregma; depth, 3 mm from dura) of female NOD/SCID mice, and 3 μL of 38C2 SNS cell suspension (2×10^5 cells) was injected. Twenty-four weeks after transplantation, the treated mice were cardially perfused, processed for immunohistochemical analysis, and analyzed by confocal laser scanning microscopy (LSM 510 META; Carl Zeiss). To distinguish Venus from EGFP, the LSM 510 META system was used.

Preparation of Mouse Whole-Dermal Fibroblasts. The whole dermis was collected from adult female C57BL/6J mice and cultured in MF-start medium (Toyobo). After lentiviral transduction with Venus (3), these cells were used for transplantation.

1. Okada Y, et al. (2008) Spatiotemporal recapitulation of central nervous system development by murine embryonic stem cell-derived neural stem/progenitor cells. *Stem Cells* 26: 3086–3098.
2. Okada Y, Shimazaki T, Sobue G, Okano H (2004) Retinoic-acid-concentration-dependent acquisition of neural cell identity during in vitro differentiation of mouse embryonic stem cells. *Dev Biol* 275:124–142.
3. Miyoshi H, Blömer U, Takahashi M, Gage FH, Verma IM (1998) Development of a self-inactivating lentivirus vector. *J Virol* 72:8150–8157.
4. Okada S, et al. (2005) In vivo imaging of engrafted neural stem cells: Its application in evaluating the optimal timing of transplantation for spinal cord injury. *FASEB J* 19: 1839–1841.
5. Ogawa D, et al. (2009) Evaluation of human fetal neural stem/progenitor cells as a source for cell replacement therapy for neurological disorders: Properties and tumorigenicity after long-term in vitro maintenance. *J Neurosci Res* 87:307–317.

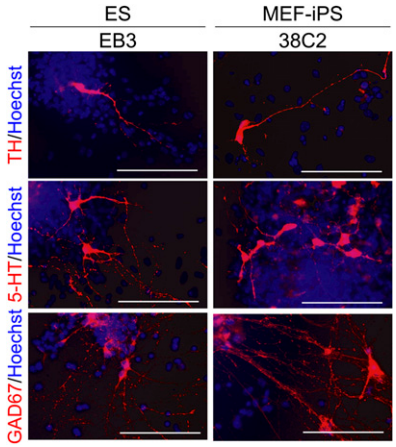

Fig. S1. Neural differentiation of pre-evaluated safe MEF-iPS cells in vitro. Immunocytochemical analyses of tyrosine hydroxylase (TH), 5-hydroxytryptamine (5HT), and glutamic acid decarboxylase 67 (GAD67) proteins in the differentiated PNSs derived from EB3 ES and 38C2 iPS cells. (Scale bar: 100 μm.)

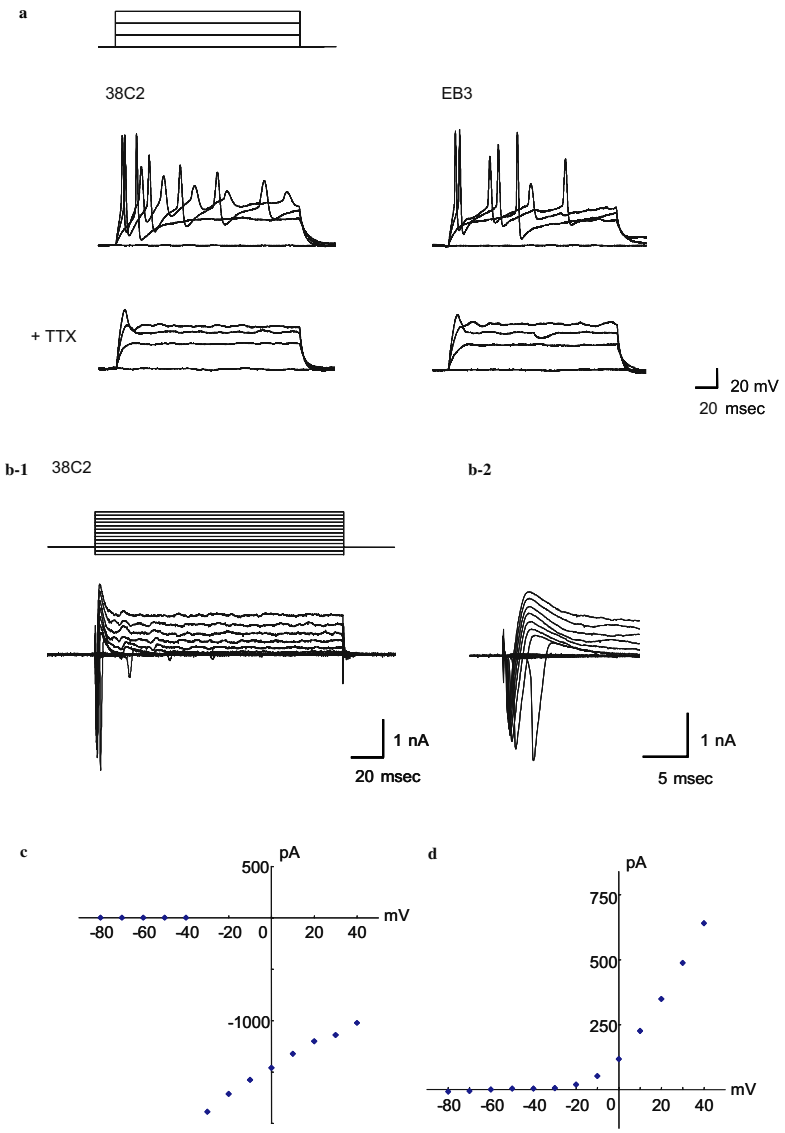

Fig. S2. Action potentials evoked in safe 38C2 iPS-derived neurons. (*A*) Positive step-current injections (25 pA, 150 ms) evoked repetitive TTX-sensitive action potentials in both 38C2 iPS- and EB3 ES-derived neurons by current clamp analyses. (*B*) Representative voltage-activated currents obtained from 38C2 iPS-derived neurons by voltage clamp analyses. (*B*-1) Currents observed when voltage steps (10 mV, 150 ms) were applied from −90 mV to 40 mV. (*B*-2) Na^+ currents observed during the initial 15 msec of the voltage steps. (*C*) *I–V* relationship for the peaks of the inward Na^+ currents in 38C2 iPS-derived neurons. (*D*) The steady-state current amplitudes plotted as the *I–V* relationship for K^+ currents in 38C2 iPS-derived neurons.

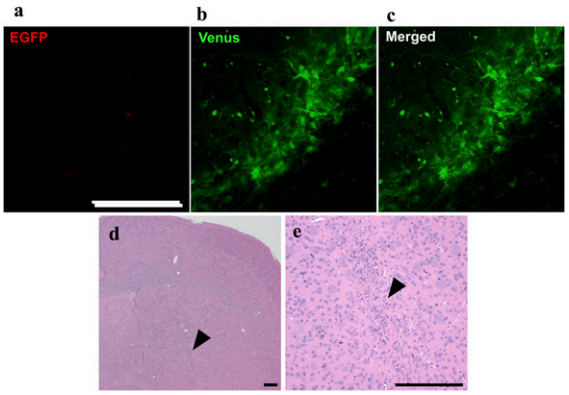

Fig. S3. No evidence of tumorigenesis in the brain of NOD/SCID mice 24 wk after the transplantation of safe 38C2 SNSs. (*A*) EGFP expression examined by META analysis. No Nanog EGFP$^+$ cell was detected. (*B*) Venus$^+$-grafted 38C2 SNSs survived. (*C*) Merged image of *A* and *B*. (*D* and *E*) H&E staining of NOD/SCID mouse brains 24 wk after 38C2 SNS transplantation. No sign of tumorigenesis was observed (*E* is magnified image of *D*). (Scale bar: *A*, 100 μm; *D* and *E*, 250 μm.) Arrowheads indicate graft sites.

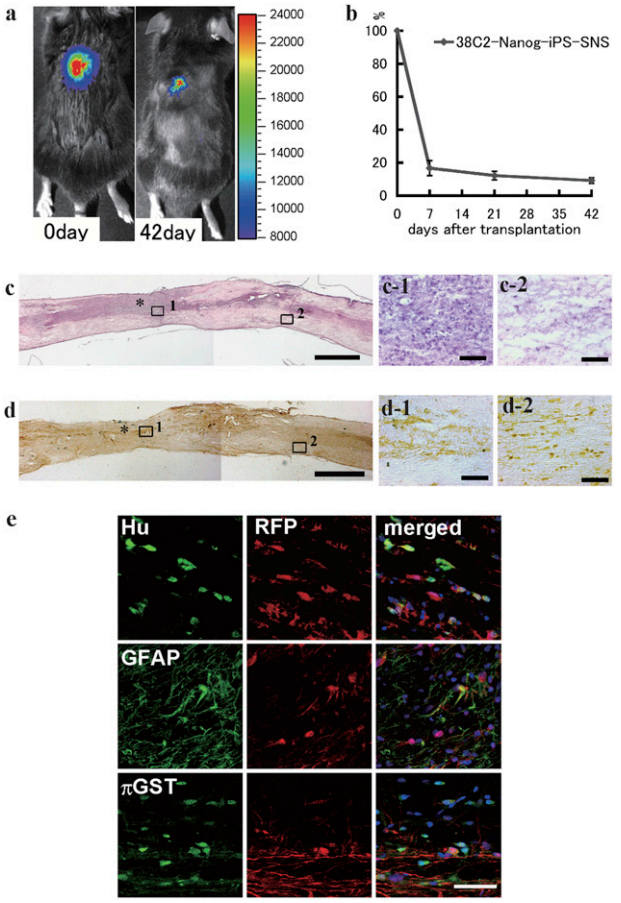

Fig. S4. Safe MEF-iPS-SNSs transplanted into intact spinal cord survive without any evidence of tumorigenesis and differentiate into three neural lineages. (*A*) Representative BLI images of a mouse transplanted with CBR*luc*-expressing 38C2 SNSs. (*Left*) Immediately after transplantation. (*Right*) Forty-two days after transplantation. (*B*) Time course of BLI photon intensity showing the viability of 38C2 SNSs transplanted into the intact spinal cord. There was a drastic reduction in signal intensity within the first 7 d after transplantation, which was followed by a relatively stable bioluminescent signal for the following 42 d. Values are means ± SEM ($n = 2$). (*C*) H&E and (*D*) anti-RFP diaminobenzidine staining of sagittal section of the spinal cord 42 d after transplantation. There was no evidence of tumorigenesis (*C*). Higher-magnification images of the boxed areas show the injection epicenter (*C*-1), and the white matter caudal to the injection site (*C*-2). There existed the grafted RFP$^+$ cell around the injection site (*D*). Higher-magnification images of the boxed areas reveal RFP$^+$ grafted cells in both the gray (*D*-1) and white matter (*D*-2) with no evidence of tumorigenesis. *Graft site. (*E*) Immunohistochemical analyses of the 38C2 SNSs grafted into the intact spinal cord 42 d after transplantation show RFP+ grafted cells that were also positive for markers of neural lineages: Hu$^+$ neurons, GFAP$^+$ astrocytes, and π-GST$^+$ oligodendrocytes. (Scale bar: *C* and *D*, lower magnification 1 mm; *C* and *D*, higher magnification, 50 μm; *E*, 50 μm.)

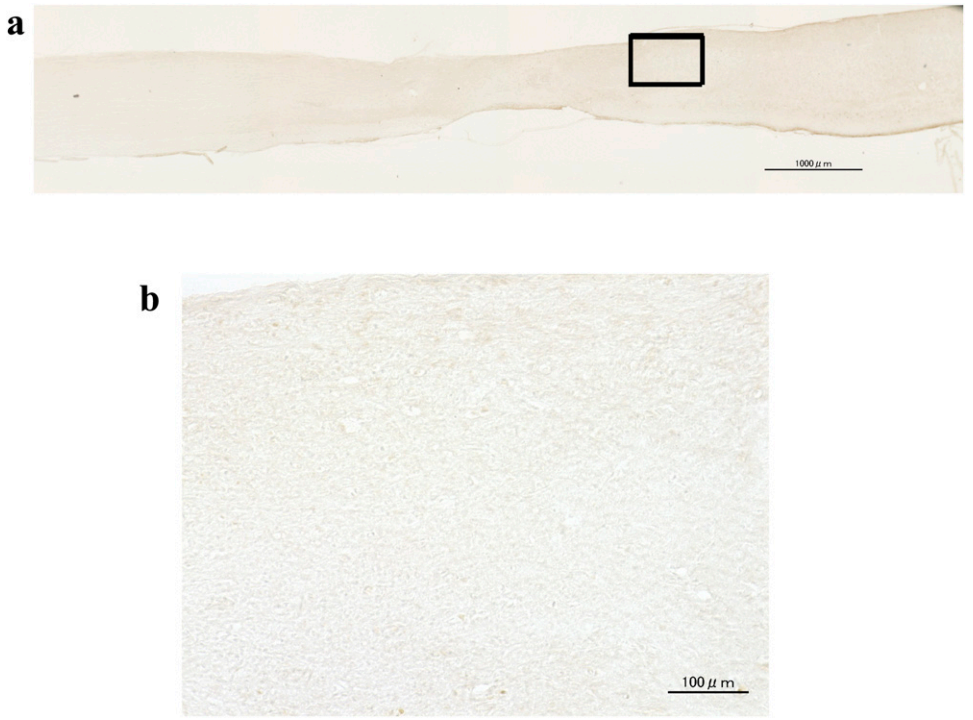

Fig. S5. No tumor formation in the 38C2 SNSs grafted spinal cords. Histological analysis of 38C2 iPS-SNS grafted spinal cord using anti-Nanog antibody. No Nanog^{+} cells were observed in the injured spinal cord 42 d after the transplantation. (*Lower*) Higher-magnification view of the boxed area of upper panel. (Scale bar: *A*, 1 mm; *B*, 100 μm.) See Fig. 5*G* for comparison.

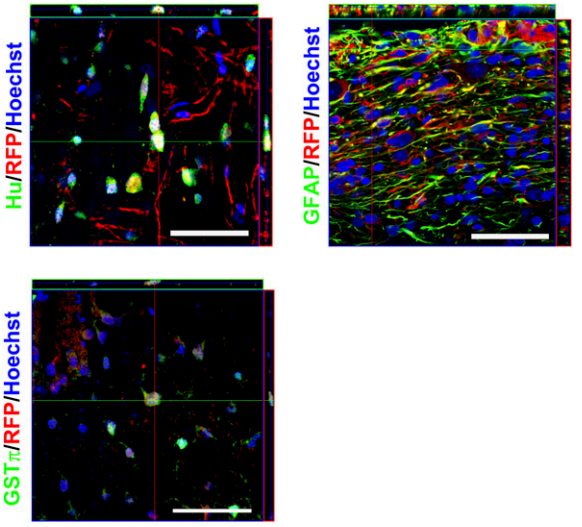

Fig. S6. Immunohistochemical images in *x-y-z* planes of the injured spinal cords after 38C2 SNSs transplantation. Reconstructed images showed that the RFP^{+} graft-derived cells are also positive for markers of neural lineages: Hu^{+} neurons, GFAP^{+} astrocytes, and GST-π^{+} oligodendrocytes. (Scale bar: 50 μm.)

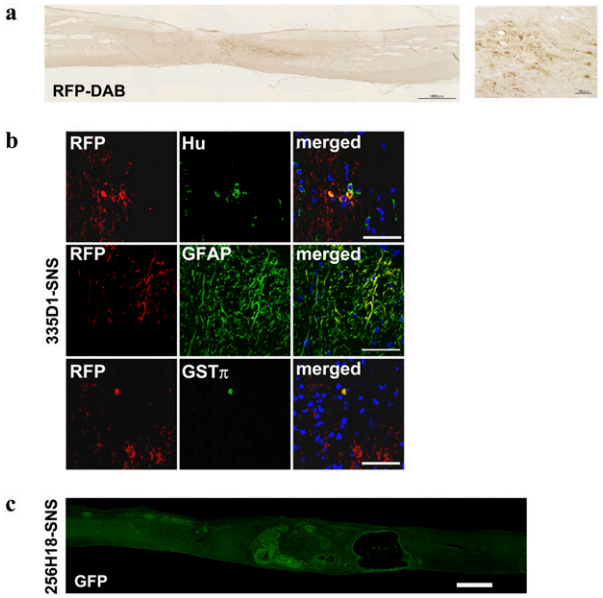

Fig. S7. Immunohistochemical analyses of the injured spinal cords after safe or unsafe TTF-iPS-SNSs transplantation. (*A*) anti-RFP DAB staining of sagittal sections of the spinal cord 42 d after injury (safe 335D1 SNS transplanted). There was no evidence of tumorigenesis. (*B*) Immunohistochemical analyses of 335D1-SNSs grafted into spinal cord 42 d after injury, revealing grafted cells double-positive for RFP and markers of neural lineages. (*C*) anti-GFP staining of sagittal section of the spinal cord 42 d after injury (unsafe 256H18 SNS transplanted). Teratomas containing EGFP$^+$ cells were observed.

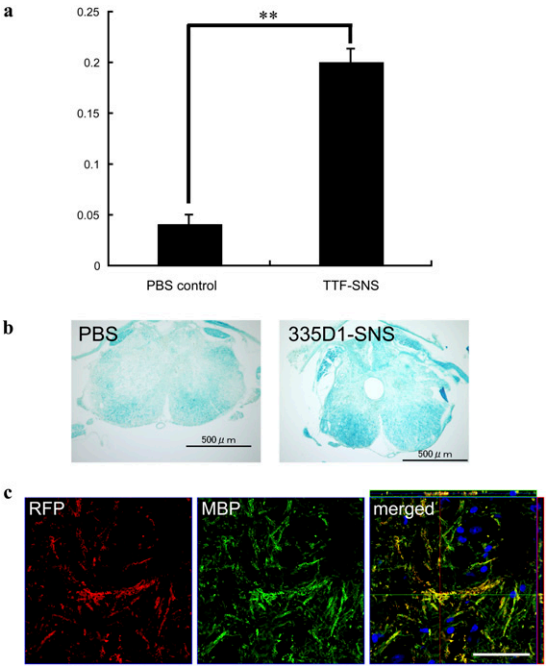

Fig. S8. Quantitative analysis of LFB$^+$ area after 335D1 SNSs transplantation. (*A*) Quantification of LFB$^+$ areas at the lesion epicenter 42 d after injury ($n = 3$ each; $^{**}P < 0.01$). (*B*) LFB staining of axial sections of the spinal cord at the lesion epicenter 42 d after injury; PBS control (*Left*) and 335D1 iPS-SNS–transplanted (*Right*) animals. (Scale bar: 500 μm.) (*C*) Immunohistochemistry of 335D1-iPS-SNS–derived mature oligodendrocytes (MBP$^+$). Grafted cells were integrated into myelin sheath. (Scale bar: 50 μm.)

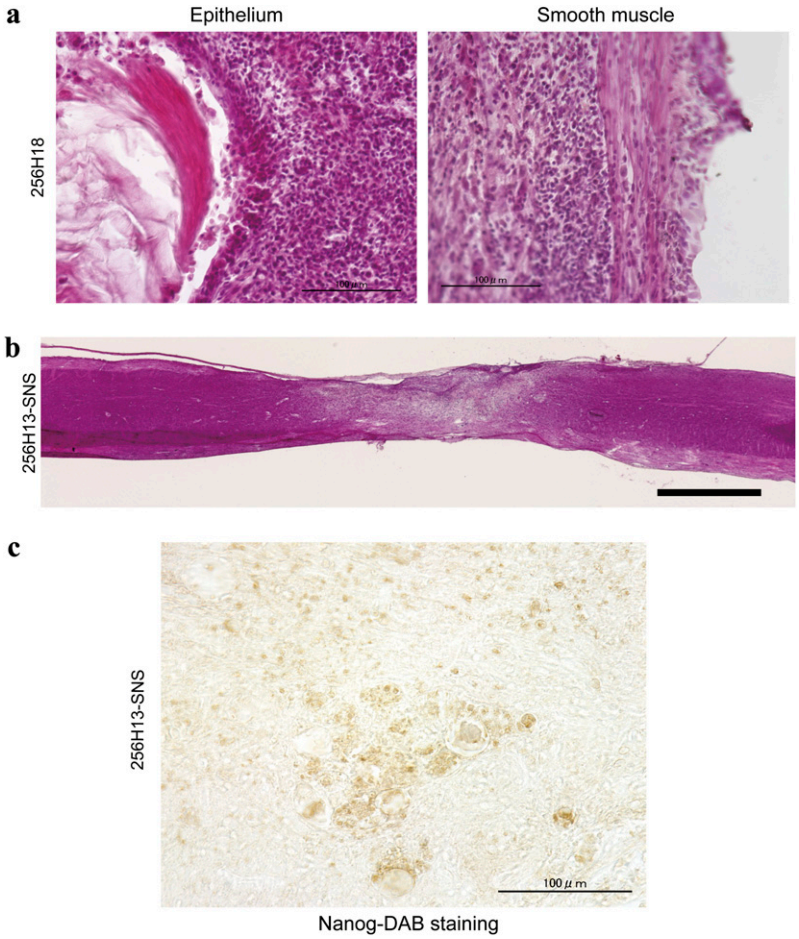

Fig. S9. (*A*) Teratoma formation in injured spinal cords after unsafe 256H18 SNSs transplantation. Higher-magnification views of Fig. 5*E*. Stratified squamous epithelia with keratinization (*Left*) and smooth muscle tissues around the dilated cyst (*Right*) were observed. (*B* and *C*) Scattered small cell clusters of Nanog$^+$ undifferentiated cells in injured spinal cords after unsafe 256H13 SNSs transplantation. Only one mouse in the 256H13 group showed teratoma formation at 6 wk after injury through H&E staining. No tumor formation was observed in the other mice in 256H13 group (*B*). However, scattered small clusters of Nanog$^+$ undifferentiated cells were observed in these mice without obvious teratoma formation (*C*). (Scale bar: *A* and *C*, 100 μm; *B*, 1 mm.)

Table S1. RT-PCR primers in this study

Gene	Sense	Antisense
Nanog	AGGGTCTGCTACTGAGATGCTCTG	CAACCACTGGTTTTTCTGCCACCG
ERas	ACTGCCCCTCATCAGACTGCTACT	CACTGCCTTGTACTCGGGTAGCTG
Oct3/4	CTGAGGGCCAGGCAGGAGCACGAG	CTGTAGGGAGGGCTTCGGGCACTT
Sox2	GGTTACCTCTTCCTCCCACTCCAG	TCACATGTGCGACAGGGGCAG
c-Myc	CAGAGGAGGAACGAGCTGAAGCGC	TTATGCACCAGAGTTTCGAAGCTGTTCG
Klf4	CACCATGGACCCGGGCGTGGCTGCCAGAAA	TTAGGCTGTTCTTTTCCGGGGCCACGA
Sox1	ATGTACAGCATGATGATGGAGACC	AGCGAGTACTTGTCCTTCTTGAGC
Tuj1	AGACCTGCAGCTGGAGCGCATCAG	CAGCTCCGCGCCCTCCGTATAGTG
GFAP	GCCCAACAGCAGGTCCACGTGGAG	AGCTTCGTGCTTGGCTTGGCGGAG
Gata6	GCAATGCATGCGGTCTCTACAGC	TCAGGCCAGGGCCAGAGCACACCAAGAATC
Brachury (T)	ATGCCAAAGAAAGAAACGAC	AGAGGCTGTAGAACATGATT
EGFP	CGACTTCTTCAAGTCCGCCATGCCCG	CCAGCAGGACCATGTGATCGCGCTTC
b-actin	CGTGGGCCGCCCTAGGCACCA	TTGGCCTTAGGGTTCAGGGGG

Table S2. Antibodies used in this study

Antibody type	Condition
For immunocytochemistry	
Tuj1 (Sigma)	Mouse IgG, 1:1,000
GFAP (DAKO)	Rabbit IgG, 1:4,000
O4 (Chemicon)	Mouse IgM, 1:5,000
CNPase (Sigma)	Mouse IgG, 1:400
5-HT (Sigma)	Rabbit IgG, 1:20,000
TH (Chemicon)	Rabbit IgG, 1:100
GAD67 (Chemicon)	Mouse IgG, 1:2,500
For immunohistochemistry of NOD/SCID mice analyses	
NeuN (Chemicon)	Mouse IgG, 1:500
GFAP (DAKO)	Rabbit IgG, 1:400
APC (Oncogene)	Mouse IgG, 1:100
GFP (MBL)	Rabbit IgG, 1:500
For immunohistochemistry of intact/injured spinal cord	
Hu*	Human serum, 1:1,000
GFAP (Zymed)	Rat IgG, 1:200
π-GST (BD Biosciences)	Mouse IgG, 1:500
5-HT (Immunostar)	Goat IgG, 1:200
NF200 (Chemicon)	Mouse IgG, 1:500
MBP (Aves Labs)	Chick IgY, 1:200
RFP (MBL)	Rabbit, 1:200
Nanog (ReproCELL)	Rabbit, 1:200

*A gift from Dr. Robert Darnell, Rockefeller University.